Incompressible Turbulent Flow Simulation of the Rotor-Stator Configuration

비압축성 Navier Stokes 방정식을 이용한
2차원 터빈 익렬내의 난류유동해석

H. W. Kim[*1] , W. G. Park[2] , Y. R. Jung[3] ,
K. S. Kim[4] , S.-G. Moon[5]
김 홍 원 , 박 원 규 , 정 영 래,
김 기 섭, 문 성 균

ABSTRACT

터빈익렬내부의 유동해석을 위해 비압축성 점성유동해석을 이용한 수치 해석 프로그램을 개발하였다. 지배방정식으로는 2차원의 비정상 비압축성 Navier-Stokes 방정식을 일반화된 곡선좌표계로 전환하여 암시적으로(implicitly) 반복적인 시간진행방법을 이용하여 유동해석을 하였다. 지배방정식의 각항들은 시간에 대해 1차의 정확도 그리고 영역에 대해서는 2차의 정확도, 대류항에 대해서는 3차의 정확도를 가지는 Upwind기법을 적용하였다. 특히, 실험적 접근이 매우 어려운 터빈의 정익과 회전하고 있는 동익과의 상호운동을 멀티블럭기법과 데이터 interface를 통해 보다 쉽게 해석할 수 있었다. 본 연구결과는 정익만을 계산한 타 연구자의 결과와의 비교시 매우 일치하였으며 물리적인 유동을 잘 파악할 수 있었다. 난류유동 해석을 위해서 Baldwin-Lomax 모델을 적용하였다.

1. INTRODUCTION

The turbine cascade flow analysis is essential to predict accurate performances of a turbine vibration, fatigue break of blade, and turbine noise. The turbine stages comprised of successive blade rows of stator and rotor are always associated with periodically unsteady flows, and these periodic changes of flow variables have a considerable effects on the turbine performances. Numerical methods for cascade flow analysis of turbine cascade range from potential equation to Navier-Stokes equation diversely. Recently, approaches of inviscid flow analysis using Euler equation and viscous flow analysis using Navier-Stokes equation have been actively studied. Erdos[1], Gile[2], and Jorgenson[3] solved Euler equation using MacCormack, Lax-Wendroff, 4th Runge-Kutta scheme, respectively. The full Navier-Stokes equations are solved by Rai[4], Hah[5], Chimma[6], etc. But, most Navier-Stokes equation solvers are based on compressible flows and are not efficient for analysis of low Mach numbers($M<0.3$) incompressible flow simulation. The major difficulty in solving incompressible Navier-Stokes is that the governing equations are a mixed elliptic-parabolic type of partial differential equations. The continuity equation does not have a time derivative term and is given in the form of a divergence-free constraint. The absence of a time derivative term in the continuity equation prohibits integration of continuity equation by a time marching scheme. The compressible Navier-Stokes equations, on the other hand, are efficiently integrated by time marching schemes because they are a set of parabolic-hyperbolic partial differential equations. The objective of present work is to apply the iterative time marching scheme for accurately and efficiently simulating 2-dimensional incompressible flow through a turbine stage.

1.2.3 Department of Mechanical Engineering Pusan National University, Pusan 609-735, KOREA
4. Korea Research Institute of Ships and Ocean Eng. Daejeon 305-606, KOREA
5.Nuclear Training Center Korea Electric Power Corporation 991, Sinam-Ri, Seasaeng-Myon Ulsan-Gun, Kyung Nam 689-880 KOREA

2. MATHEMATICAL AND NUMERICAL FORMULATIONS

2.1 GOVERNING EQUATIONS

Two-dimensional unsteady incompressible Navier-Stokes equations in an generalized curvilinear coordinate system may be written as follows :

$$\frac{\partial \hat{q}}{\partial t}+\frac{\partial}{\partial \xi}(\hat{E}-\hat{E}_v)+\frac{\partial}{\partial \eta}(\hat{F}-\hat{F}_v)=0 \tag{1}$$

where $\hat{q}$, $\hat{E}$, $\hat{F}$, $\hat{E}_v$, $\hat{F}_v$ are flux vectors defined as

$$\hat{q}=\frac{1}{J}\begin{bmatrix}0\\u\\v\end{bmatrix} \tag{2}$$

$$\hat{E}=\frac{1}{J}\begin{bmatrix}U-\xi_t\\uU+p\xi_x\\vU+p\xi_y\end{bmatrix},\quad \hat{F}=\frac{1}{J}\begin{bmatrix}V-\eta_t\\uV+p\eta_x\\vV+p\eta_y\end{bmatrix}$$

and

$$\hat{E}_v=\frac{1}{JRe}\begin{bmatrix}0\\(\nabla\xi\cdot\nabla\xi)u_\xi+(\nabla\xi\cdot\nabla\eta)u_\eta\\(\nabla\xi\cdot\nabla\xi)v_\xi+(\nabla\xi\cdot\nabla\eta)v_\eta\end{bmatrix}, \tag{3}$$

$$\hat{F}_v=\frac{1}{JRe}\begin{bmatrix}0\\(\nabla\eta\cdot\nabla\xi)u_\xi+(\nabla\eta\cdot\nabla\eta)u_\eta\\(\nabla\eta\cdot\nabla\xi)v_\xi+(\nabla\eta\cdot\nabla\eta)v_\eta\end{bmatrix},$$

The contravariant velocities U and V are defined as

$$U=\xi_t+u\xi_x+v\xi_y$$
$$V=\eta_t+u\eta_x+v\eta_y$$

Here J is the Jacobian of transformation and the quantities ξ_t and η_t are presented for the grid motion of the rotor. These quantities are given in terms of the velocity of the grid (x_τ, y_τ) with reference to a stationary observers :

$$\xi_t=-x_\tau\xi_x-y_\tau\xi_y \tag{4}$$
$$\eta_t=-x_\tau\eta_x-y_\tau\eta_y$$

2.2 ITERATIVE TIME MARCHING PROCEDURE

The goal of present procedure is to advance the flow properties(p, u, v) from a known time level 'n' to the next time level 'n+1'. First of all, let us consider the momentum equation. Since the momentum equation is a parabolic type of partial differential equation, it can be solved using a time marching scheme as follows :

$$\frac{1}{\Delta\tau}(\bar{q}^{n+1}-\bar{q}^n)+\delta_\xi\bar{E}^{n+1}+\delta_\eta\bar{F}^{n+1}=\delta_\xi\bar{E_v}^{n+1}+\delta_\eta\bar{F_v}^{n+1} \tag{5}$$

where the barred quantities are the same quantities of Eq.(2) excluding the first row element. For example,

$$\hat{q}=\frac{1}{J}\begin{bmatrix}u\\v\end{bmatrix}\quad;\quad \hat{E}=\frac{1}{J}\begin{bmatrix}uU+p\xi_x\\vU+p\xi_y\end{bmatrix} \tag{6}$$

The above discretization of Eq(5) is the first order accurate in time. But, extension to second

order accurate in time easily achievable by replacing the first term of LHS in Eq.(5) by $(3\,\bar{q}^{n+1} - 4\bar{q} + \bar{q}^{n-1}) / 2\Delta t$. The operators, δ_ξ and δ_η represent spatial differences. If Newton iteration method is applied to solve this unsteady flow problem, Eq.(5) is rewritten as follows :

$$\frac{1}{\Delta\tau}(\bar{q}^{n+1,k+1} - \bar{q}^{n}) + \delta_\xi \bar{E}^{n+1,k+1} + \delta_\eta \bar{F}^{n+1,k+1} = \delta_\xi \bar{E}_v^{n+1,k+1} + \delta_\eta \bar{F}_v^{n+1,k+1} \tag{7}$$

Following a local linearization of $\bar{E}$, $\bar{F}$, $\bar{E}_v$ and $\bar{F}_v$ about the 'n+1'time level and at the 'k' iteration level,

$$\left(\frac{I}{\Delta\tau} + \frac{\partial}{\partial\xi}A + \frac{\partial}{\partial\eta}B\right)\Delta\bar{q} = w\,\bar{R}^{n+1,k} \tag{8}$$

where ω is relaxation factor and A, B are Jacobian matrices of the flux vectors $\bar{E} - \bar{E}_v$, $\bar{F} - \bar{F}_v$ respectively :

$$A = \frac{\partial(\bar{E} - \bar{E}_v)}{\partial\bar{q}}; \qquad B = \frac{\partial(\bar{F} - \bar{F}_v)}{\partial\bar{q}}; \tag{9}$$

and $\bar{R}^{n+1,k}$ is the residual vector, defined as :

$$\bar{R}^{n+1,k} = -\frac{\bar{q}^{n+1,k} - \bar{q}^{n}}{\Delta\tau} - (\delta_\xi \bar{E}^{n+1,k} + \delta_\eta \bar{F}^{n+1,k} + \delta_\xi \bar{E}_v^{n+1,k} + \delta_\eta \bar{F}_v^{n+1,k}) \tag{10}$$

Note that LHS of Eq. (10) is the same form of discretized momentum equations, Eq.(5), at 'k' iteration level and when $\bar{R}^{n+1,k}$ goes to zero, the momentum equations in their discretized form are exactly satisfied at each physical time step. The solution is independent of ω, and any approximations made in the construction of A, B and C. Next, let's consider the continuity equation. As mentioned before, in order to solve incompressible viscous flow problems efficiently, we need a relationship coupling changes in the velocity field with changes in the pressure field while satisfying the divergence-free constraint. In the present study, the Marker-and-Cell (MAC) approach[7] is used to link the iterative changes between pressure and velocity, and can be written in curvilinear coordinate system :

$$\Delta\left(\frac{p}{J}\right) = -\beta\left[\frac{\partial}{\partial\xi}\left(\frac{U-\xi_t}{J}\right) + \frac{\partial}{\partial\eta}\left(\frac{V-\eta_t}{J}\right)\right]^{n+1,k} \tag{11}$$

where $\Delta(p/J) = (p/J)^{n+1,k+1} - (p/J)^{n+1,k}$ and β is a relaxation factor, that may even vary from node to node as in a local time concept. Again, when Δq goes to zero, the continuity equation is exactly satisfied at each time step, even in unsteady flows. Eq.(11) states that if a cell is accumulating mass, then the pressure value at the next iteration is increased to repel fluid away from the cell. If a cell is losing mass, then the pressure value is lowered to draw fluid. Thus the pressure field is iteratively updated along with the velocity field until the conservation of mass is satisfied. The spatial derivatives of convective flux terms are differenced by using third order accurate upwind QUICK (Quadratic Upstream Interpolation For Convection Kinematics) scheme[8] to reduce unphysical oscillations for high Reynolds number flows, and the spatial derivatives of viscous terms are differenced using half-point central differencing. The spatial derivatives of continuity equation is differenced with central differencing and a fourth order artificial damping term is added to the continuity equation to stabilize the present procedure. Combining the momentum equation, Eqn. (8) and the continuity equation Eqn. (11), and applying the numerical discretization in time and space at all nodes in the flow field, a system of simultaneous equation results for the quantity $\Delta\hat{q}$ equal to

$(\Delta\frac{p}{J}, \Delta\frac{u}{J}, \Delta\frac{v}{J})$. The system may be formally written as :

$$[M]\ \{\Delta q\} = \{R\} \tag{12}$$

Here, since the right hand side $\{R\}$ is the discretized form of the unsteady governing equations, as long as $\{\Delta q\}$ is driven to zero, the discretized form of unsteady Navier-Stokes equation are exactly satisfied at physical time level '$n+1$' . The steady state solutions are obtained as asymptotic solutions of the time marching process. Although the matrix [M] is a sparse and banded matrix, direct inversion of this matrix requires a huge number of arithmetic operations. A common strategy in iterative solutions of elliptic equations is to approximate the matrix [M] by another, easily inverted matrix [N]. In this study, matrix [N] contains only the diagonal contributions of matrix [M], and Eq.(12) becomes an explicit form which is easier to be tailored for efficient execution on the current generation of vector or massively parallel computer architectures than an implicit form. The flowfield over stator-rotor configuration has viscous nature with complex features like interaction between stator and rotor and interactions between trailing edge and boundary layer induced by suction side, etc. Flow separation and reattachment may also be present. To capture these flow details, a viscous simulation with a suitable turbulence model is essential. In present work, the modified Baldwin-Lomax model is implemented.

3. SLIDING MULTI-BLOCK TECHNIQUE

Since it is hard to generate a single grid system about very complex geometries, a domain decomposition techniques are widely used. In this method, the overall domain is subdivided into several blocks. In each block, a grid is generated separately and the flowfield is solved independently of the other blocks. The boundary data for each block is provided by the neighboring blocks. The present work decomposed the whole domain into four blocks as shown in Fig. 1. The body-fitted H-grid is generated using elliptic partial equation[11] for orthogonality and mesh-point clustering near the turbine stage boundary. Each block has 95× 51 grid points. Block #1 and 2 for the stator is stationary while block #3 and 4 for the rotor is moving downward at given translational velocity. Therefore, the interpolation at block interfaces between block #1, 2 and block #3, 4 is needed while satisfying the conservation properties. A schematic of the grid at the interface boundary between stator and rotor is shown in Fig. 2. Because block #3, 4 is sliding down, there is discord of bock interface line. The present interpolation technique is followed by the method of Srivastava[10]. First, the sliding interface boundary of the block #3, 4 is updated using the present iterative time marching scheme. In order to update the flow properties at the node B(refer to Fig. 2), the grid line AB is extended until it intersects the plane I=Imax-1 of the second block at point C. The flow properties are then obtained at point C by interpolating from the flow properties of the I=IMAX-1 plane using a Lagrangian polynomial interpolation. The node B is then updated by taking the linearity of the values at node A and point C. But, in contrast to point B, it seems that the node F cannot be extended to first block. Here the node F is updated by using periodic condition. This process is repeated for all the nodes associated with I=1 plane of the third and fourth block. Then all the node of block #1, and block #2 (eg. G, H, etc) is obtained from updated flow properties of block #3, 4 by using interpolation.

4. INITIAL AND BOUNDARY CONDITIONS

The governing equations are always solved in the inertial frame. The use of inertial frame simplifies the governing equations because the centrifugal and Coriolis forces do not appear explicitly. This approach is suitable for rotating blade or turbomachinery. The governing

equation (1) requires initial conditions to start the calculation as well as boundary condition at every time step. In present work, the quantities Δp, Δu and Δw are initially set to zero at all solid and fluid boundaries. The boundary values as well as interior values are iteratively advanced from a time level 'n' to 'n+1'. On solid surface, the no slip condition is imposed for velocity components. The surface pressure distribution is determined by setting the normal gradient of pressure to be zero. The outflow boundary condition is obtained by which pressure is freestream infinity, p_∞, and velocity is extrapolation from the interior points. Since the flow is periodic from blade to blade, the periodic condition is used on each block interfaces of passage boundary. The unsteady state calculation is started after the steady flow is fully developed.

5. RESULT AND DISCUSSION

Fig. 1 shows body fitted grid elliptically generated around a VKI stator-rotor configuration. The block number 1 and 2 is for the stator and is stationary. The block number 3 and 4 is for the rotor and is moving downward at given translational velocity. Fig. 3 shows velocity vector distribution in steady state, that is, both the stator and the rotor are stationary. The small reversed flow region near the trailing edge was found. The steady state solution agrees well to Kim's numerical results[12]. From this figure, it is shown that velocity is accelerated from leading edge at suction side of stator, however, in pressure side velocity is accelerated apparently after 40% chord. In both side, rapid acceleration and sudden deceleration at near trailing edge is resulted from large curvature variety of elliptic-type. The velocity vectors for the rotor in steady state is shown in Fig. 3(c) and (d). The small reversed region near trailing edge of the rotor is also shown. The surface pressure distribution on the stator and rotor surface is shown in Fig. 4. After the steady state solution is fully converged, the unsteady state calculation is started. Fig. 5 shows the velocity vectors at several non-dimensional time elapsed. Fig. 6 shows the velocity vectors and streamlines near the leading edge of the rotor and shows the physics of the generation of the leading edge vortex, its growing, and eventually busting of the leading edge vortex. The velocity vectors near the trailing edge of the rotor at several time elapsed is shown in Fig. 7. And the completely unsteady state motions of flowfield is found due to the relative motion of the rotor. Fig. 8 shows the surface pressure distribution on the stator and rotor surface. Compared with Fig. 4 form steady state solution, the variation of surface pressure in the rotor part is much significant and this make the flow through a turbine stage purely unsteady.

6. CONCLUSIONS

The numerical procedure has been developed for simulating incompressible turbulent flow around a turbine stage. The governing equations of 2-D unsteady incompressible Navier-Stokes equations are cast into the generalized curvilinear coordinate system and then solved implicitly. For the accurate and efficient incompressible flow analysis, the iterative time marching scheme having first order accurate in time and second to third accurate in space was applied. The sliding multiblock technique is applied to handle a relative motion of a rotor to the stator. The special treatments on these sliding block interfaces is needed to maintain the conservative properties. The turbulent flows have been modeled by the modified Baldwin-Lomax model. From present study, characteristics of flows of turbine stage which consist of stator and sliding rotor were considerably well analyzed.

7. REFERENCE

[1] J . I. Erdos, "Numerical Solution of Periodic Transonic Flow through a Fan Stage," AIAA J., Vol. 15, No. 11, 1977, pp. 1559-1568

[2] M. B. Gile, "Stator/Rotor Interaction in Transonic Turbine," AIAA-88-3093

[3] Philip C. E Jorgenson, "Explicit Runge-Kutta Method for Unsteady Rotor/Stator Interaction," AIAA J., Vol. 27, No. 6, 1989, pp 743-749

[4] Rai, M. M., "Unsteady Three-Dimensional Navier-Stokes Simulations of Turbine Rotor-Stator Interactions", AIAA Paper 87-2058, 1987.

[5] Hah, C., "A Navier-Stokes Analysis of Three-Dimensional Turbulent Flows Inside Turbine Blade Rows at Design and Off-Design Conditions," J. of Eng. for Gas Turbines and Power, Trans, ASME, Vol. 106, pp. 421-429, 1984.

[6] Chima, R. V. and Yokota, J. W., "Numerical Analysis of Three-Dimensional Viscous Internal Flows," AIAA J., Vol, 28, No. 5, pp. 798-806, 1990.

[7] Viecelli, J. A., "A Method for Including Arbitrary External Boundaries in the MAC Incompressible Fluid Computing Technique," Journal of Computational Physics, Vol. 4, 1969, pp. 543-551.

[8] Leonard, B. P., "A Stable and Accurate Convective Modeling Procedure Based on Quadratic Upstream Interpolation," Computer Methods in Applied Mechanics and Engineering, Vol. 19, 1979, pp. 59-98.

[9] W. G. Park and Sankar, L. N., "A Technique for the Prediction of Unsteady Incompressible Viscous Flows," AIAA Paper 93-3006, 1993.

[10] Srivastava, R., "An Efficient Hybrid Scheme for the Solution of Rotational Flow Around Advanced Propellers," Ph. D. Thesis, Georgia Institute of Technology, Atlanta, Georgia, August 1990.

[11] Steger, J. L. and Sorenson, R. L., "Automatic Mesh-Point Clustering Near a Boundary in Grid Generation with Elliptic Partial Differential Equations, Journal of Computational Physics 33, 405-410 1979.

[12] G. S. Kim, K. C. Kim and M. Y. Hah., "Development of Flow Analysis Program for Turbine Design", report sponsored by Han-Kook Heavy Industry, 1995.

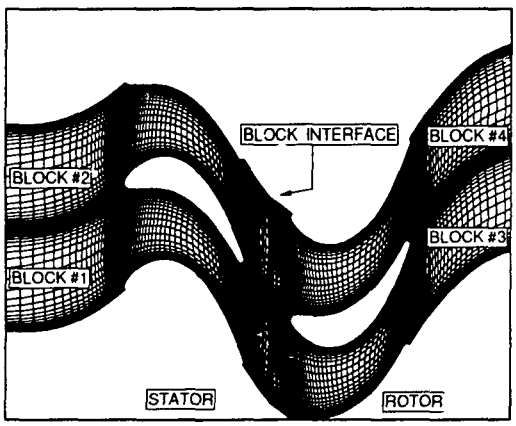

Figure 1. Stator and Rotor configuration of VKI model

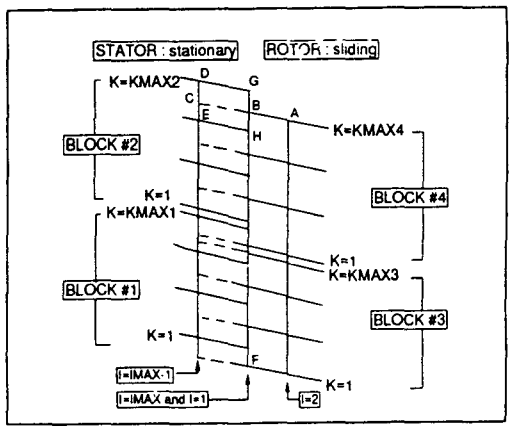

Figure 2. The treatment of multiblock interface boundar

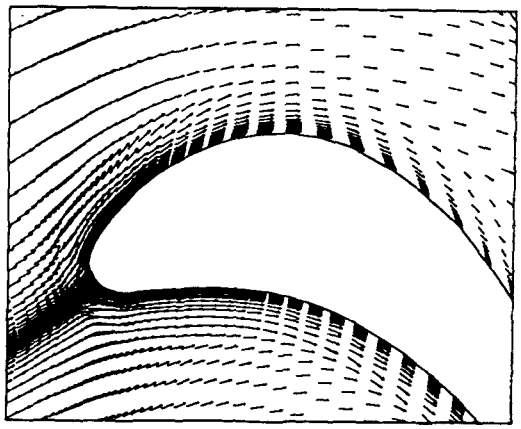

(a) near the leading edge of the stator

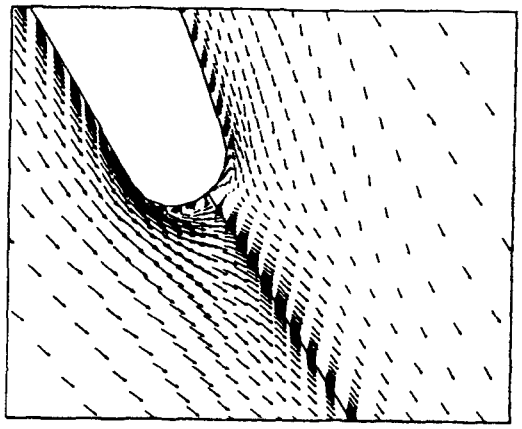

(b) near the trailing edge of the stator

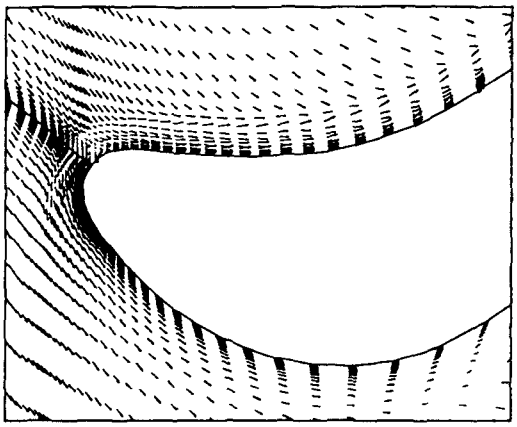

(c) near the leading edge of the rotor

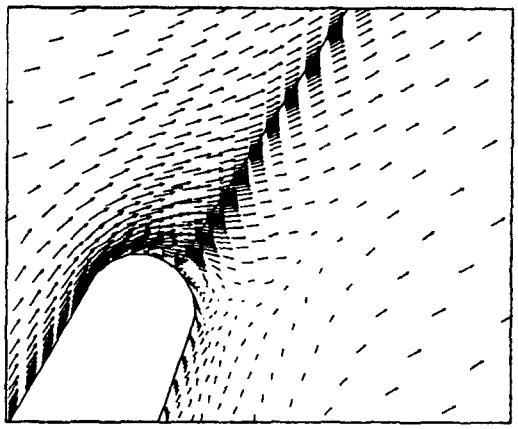

(d) near the trailing edge of the rotor

Figure 3. Velocity vectors in the steady state (Rotor : stationary)

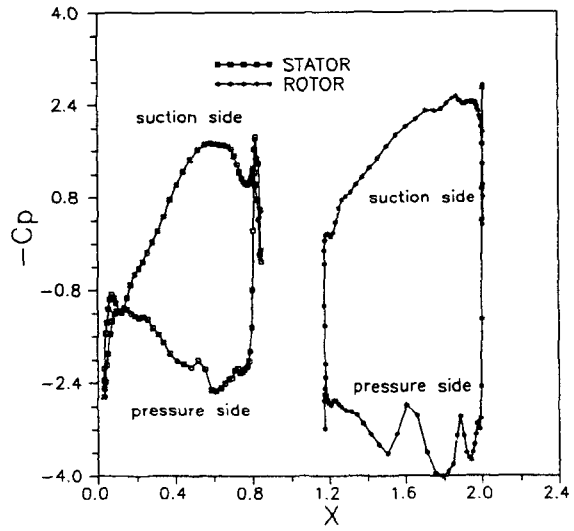

Figure 4. Surface pressure distribution on the rotor and stator surface in steady state

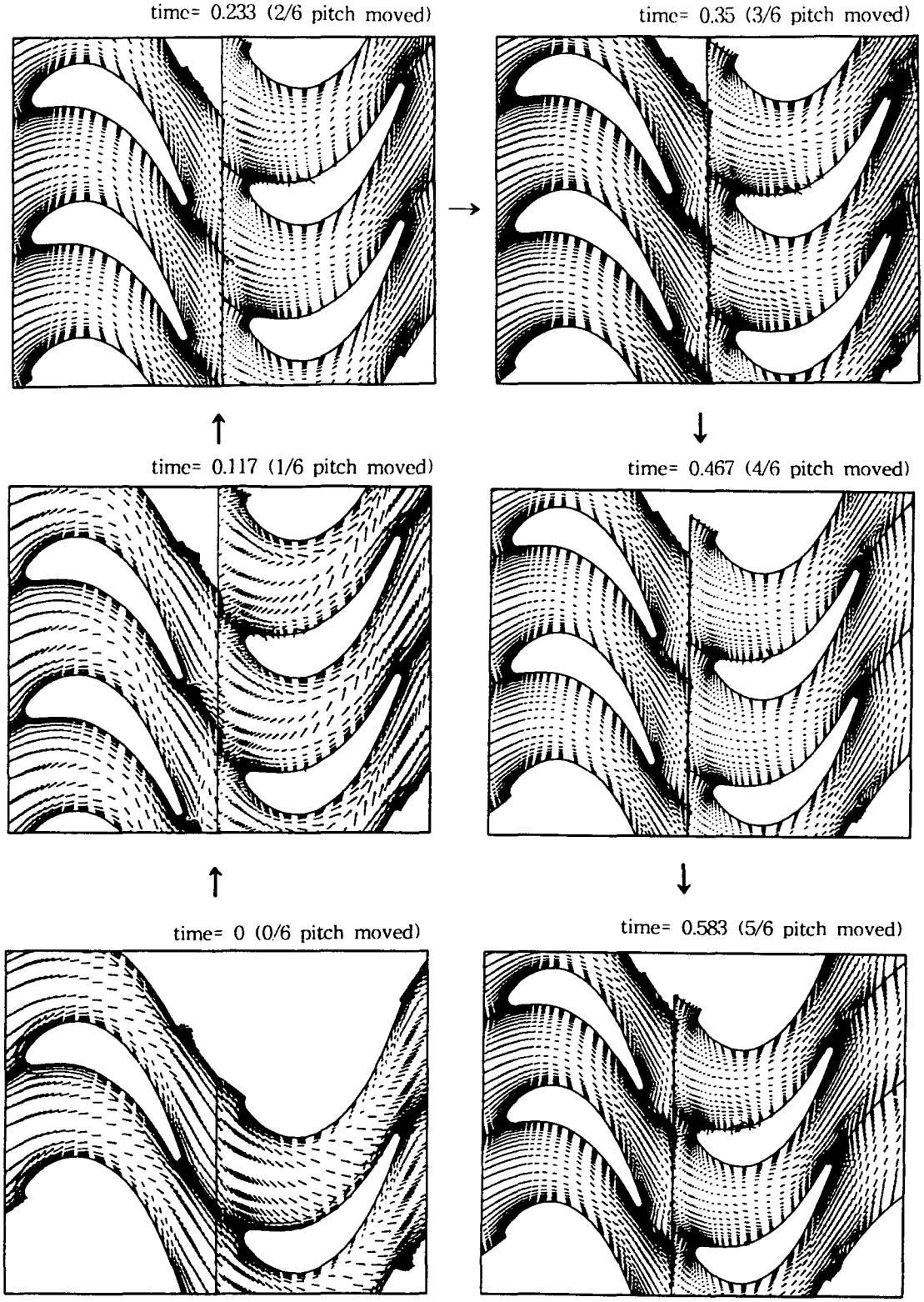

Figure 5. Velocity vectors from the unsteady state solution (Rotor : moving downward)

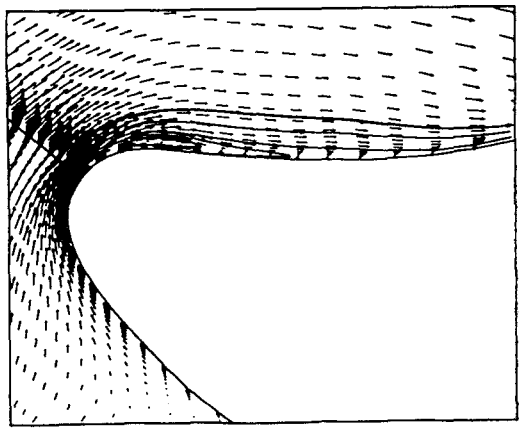

(a) at time = 0.35

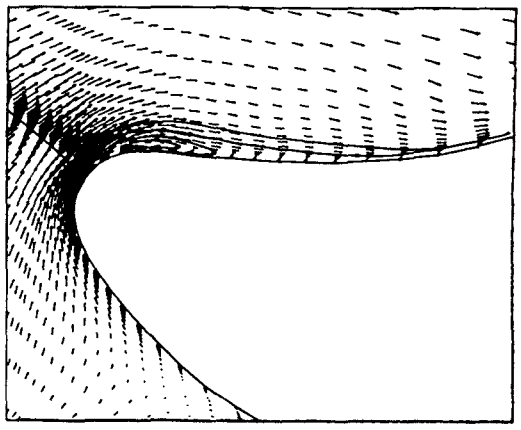

(b) at time = 0.467

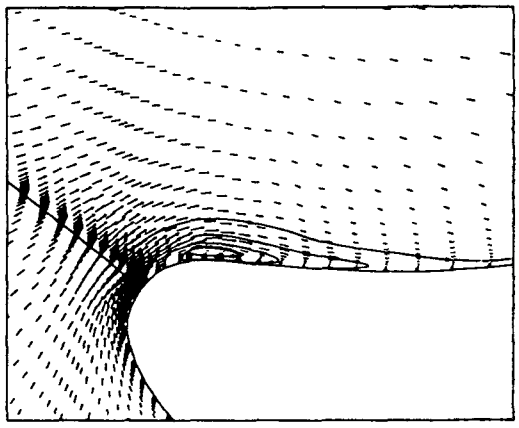

(c) at time = 0.583

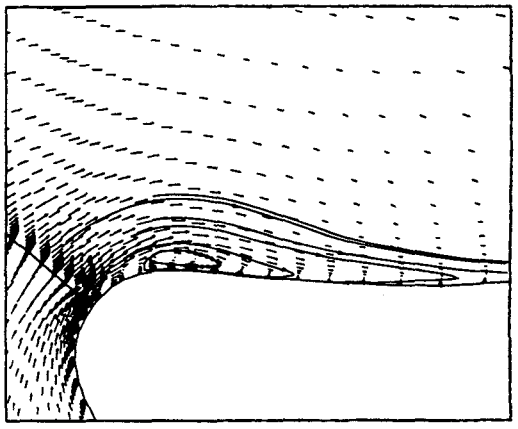

(d) at time = 0.59

Figure 6. Velocity vectors near the leading edge vortex in unsteady state

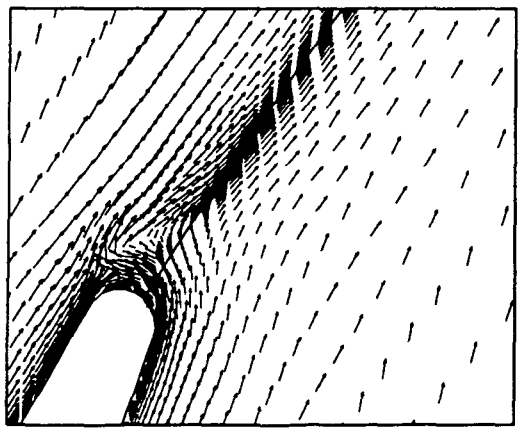

(a) at 1/6 pitch moved

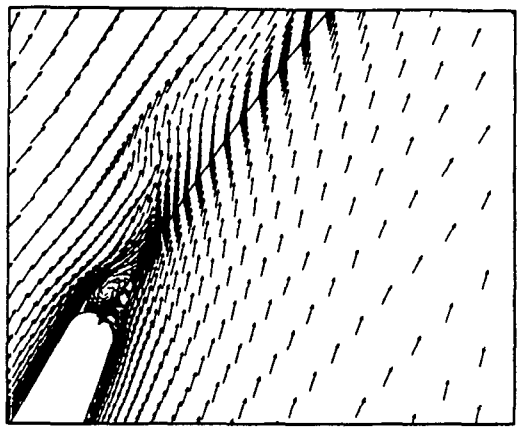

(b) at 3/6 pitch moved

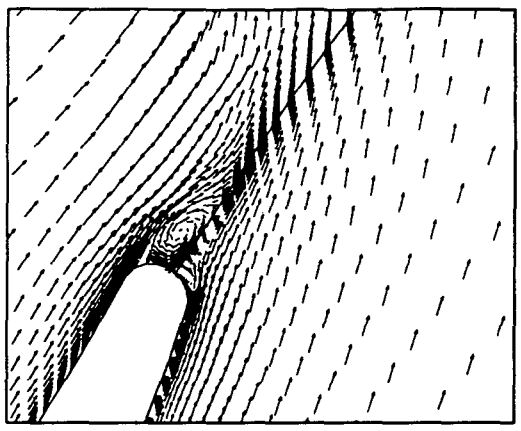

(c) at 4/6 pitch moved

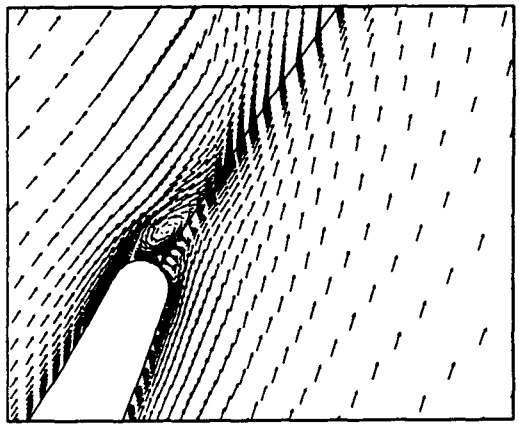

(d) at 5/6 pitch moved

Figure 7. Velocity vectors changes at near trailing edge of rotor as the rotor moves downward

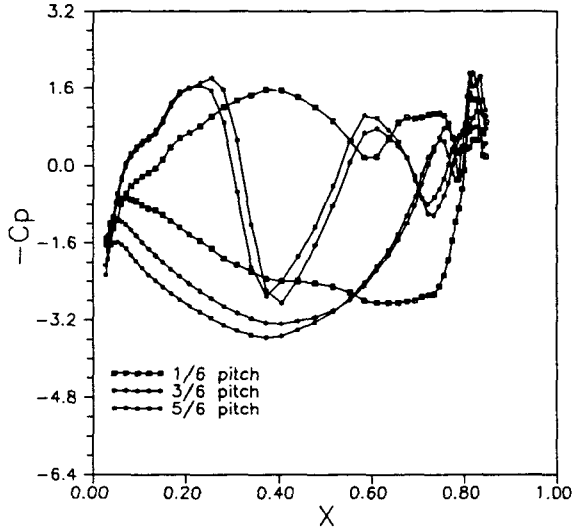

(a) stator

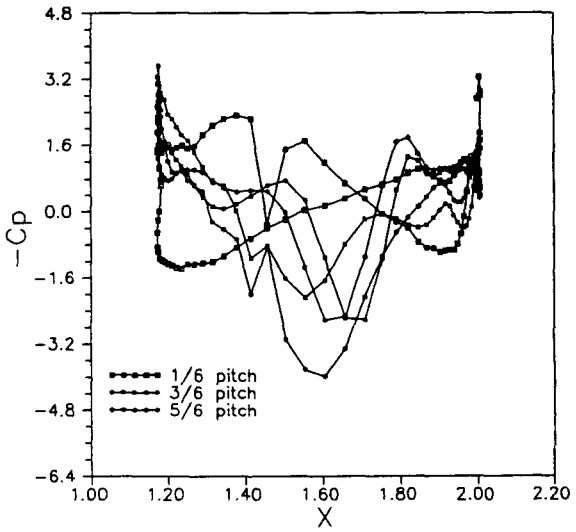

(b) rotor

Figure 8. Surface pressure distribution at several pitch moved on the rotor and stator in unsteady state